Gels

DOI: 10.1002/ange.201008182

Tunable Angle-Independent Structural Color from a Phase-Separated Porous Gel**

*Naomi Kumano, Takahiro Seki, Masahiko Ishii, Hiroshi Nakamura, and Yukikazu Takeoka**

In the natural world, there exist many sources of inspiration for the creation of new high-performance materials. Structural color observed in various creatures, plants, and minerals has received a great amount of attention in recent years because of its eye-catching, non-photobleachable, and energy-saving properties, which are important for developing unprecedented coloring materials. One of the most popular methods to obtain artificial structurally colored materials is the elaboration of periodic dielectric structures on a length scale that is comparable to the wavelength of light in materials and thus causes multiple Bragg reflections. However, the fabrication of such mesoscale structures requires a great amount of time, effort, and, in some cases, cost when using existing top-down or bottom-up approaches. Herein, we demonstrate a facile self-assembly approach to obtain a porous gel exhibiting angle-independent structural color using a principle different from that of traditional dielectric periodically structured materials. The channel-like porous structure in the gel might be self-assembled from the phase-separated polymers that result from spinodal decomposition and it might be locked in by kinetic arrest, likely through entanglement or cross-linking. The porous swollen gel changes color reversibly with solvent, covering the whole visible region in response to solvent composition and temperature by means of changes in the wavelength dispersions of the refractive indices of the gel portion and the solvent portion in the pore.

Structural color is generally defined as coloration caused by complicated and diverse interactions between light and materials, such as interference effects, diffraction grating, light scattering, and dispersion of refractive index, and it essentially does not lose the energy of the light.[1–3] For the reason, structural color has been the subject of extensive studies for applications in energy saving mobile devices with a reflective full-color paperlike display. Though structural coloration can be caused by not only periodic dielectric structures but also randomly dispersed particles and a simple prism, recent studies of artificial structurally colored materials have focused mainly on the fabrication of periodical microstructures, such as multilayer films[4–6] and photonic crystals.[7–9] This trend is in part due to the relative ease to understand the structures, and the simple principle of Bragg diffraction, which generates structural color from periodic dielectric structures. However, to design a reflective full-color paperlike display with a wide viewing angle, the angle dependence of the structural color based on Bragg diffraction becomes a major issue.

Recently, we demonstrated for the first time that amorphous arrays with a short-range order prepared from submicrometer spherical colloidal gel particles[10] or silica colloidal particles[11] are capable of displaying angle-independent structural color and can be applied to nonfading color materials and full-color paperlike displays. Theoretical interpretations for the existence of a photonic band gap causing structural color in amorphous array systems were also provided by some groups.[12,13] Counterintuitively, however, the practical fabrication of amorphous arrays from colloidal particle suspensions is a more complicated task than expected and is one of the most important challenges for large-scale production.

On this issue, living matter may give us a hint. Analogous structures and the principle of structural coloration are also found in some living matter.[14,15] For example, the amorphous packing of submicrometer spheres or tortuous channels composed of β-keratin and air nanostructures found in the feather barbs of birds produce vivid structural color without angular dependence. The structural color of the feather barbs may be produced by wavelength-selective scattering of light from the nanostructures with a short-range order, which must rely on the same principle as the above-described artificial systems. According to Dufresne, Prum, and co-workers,[14] the nanostructures in feather barbs are self-assembled by the phase separation of β-keratin from a cellular cytoplasm; the polymerization of β-keratin drives the phase separation within a cell, and arrest of the phase separation is facilitated by the entanglement or cross-linking of β-keratin filaments. As the molecular weight of β-keratin filaments increases, the entropic incentive for mixing drops, and the phase boundary shifts to higher temperatures, resulting in phase separation. If nucleation and growth occur, the system forms a submicrometer sphere-type nanostructure. When the phase separation is preceded by spinodal decomposition, a tortuous channel type nanostructure can evolve spontaneously.

This assumption stimulated our interest in fabricating such phase-separated structures by self-assembly approaches for artificial structurally colored materials. Therefore, our initial target was a biomimetic, facile preparation of self-

[*] N. Kumano, Prof. T. Seki, Prof. Y. Takeoka
Department of Molecular Design & Engineering, Nagoya University
Furo-cho, Chikusa-ku, Nagoya, 464-8603 (Japan)
E-mail: ytakeoka@apchem.nagoya-u.ac.jp
Dr. M. Ishii, Dr. H. Nakamura
Toyota Central R&D Laboratories, Inc.
Nagakute, Aichi 480-1192 (Japan)

[**] Y.T. gratefully acknowledges financial support from the Industrial Technology Research Grant Program in 2008 from the New Energy and Industrial Technology Development Organization (NEDO) of Japan (Grant 08C46502d).

Supporting information for this article is available on the WWW under http://dx.doi.org/10.1002/anie.201008182.

assembled nanostructured and structurally colored materials with short-range order on a length scale that is comparable to the wavelength of visible light. However, the self-assembled fabricated channel-type porous gel revealed unexpected tunable structural color in response to solvent composition and temperature even though the average domain size in the porous gel was much larger than the wavelength of visible light. Herein, we explain our new discovery about the facile preparation of the angle independent structural colored material and its reversible tuning coloration depending on the solvent composition and the environmental temperature.

The microstructure in the porous gel was self-assembled by phase separation of poly{2-(2-methoxyethoxy)ethyl methacrylate} [poly(MEO2)] along with reversible deactivation radical polymerization, the so-called atom transfer radical polymerization (ATRP)[16,17] that is an example of a living radical polymerization, of MEO2 using 2-bromopropionic acid butyl ester as an initiator and the CuBr/4,4′-dinonyl-2,2′-dipyridyl catalytic system without solvent below 20 °C (Figure 1). Above a reaction temperature of 50 °C, the gels obtained were transparent and homogeneous. The resulting

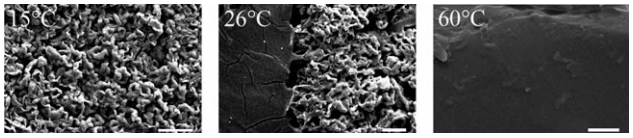

Figure 1. SEM images of gels prepared at various temperatures. Scale bars: 50 μm.

gels at a reaction temperature between 20 °C and 50 °C were mixtures of the phase-separated portion and the homogeneous portion. These results indicate that the polymerization-induced phase-separation mechanism is an upper critical solution temperature behavior.[18] As the molecular weight of poly(MEO2) increases as a result of ATRP, the position of the phase boundary shifts to higher temperature over time, and the phase separation by spinodal decomposition or nucleation and growth can proceed. Judging from the channel-type morphology of the phase-separated microstructure observed in the gel, the phase separation might be induced by spinodal decomposition. The resultant gel swells slightly in toluene, which is a good solvent for poly(MEO2) (Figure S8a in the Supporting Information), but the microstructure is almost maintained, despite the lack of a cross-linker. The unstable phase-separated microstructure is probably locked in by kinetic arrest, likely through the entanglement or cross-linking of poly(MEO2). As a result, the microstructure consists of isotropic, tortuous, and twisting channels with a characteristic length of about 10 μm, which is considerably larger than the wavelength of visible light. The size of a scattering substance is parameterized by the ratio of its characteristic length r and the wavelength of light λ as $\alpha = 2\pi r/\lambda$.[19] If the value of α becomes sufficiently larger than 1, the geometrical optic approximation can be applied to evaluate the interaction between the light and the scattering substance. Consequently, we must be able to treat this porous gel as a diffuse reflective material.

Figure 2a shows the transmission spectra of the porous gel in toluene/acetone mixed solvents at 20 °C. A quite broad peak at around 766 nm is observed from the porous gel in pure toluene. However, the color of the porous gel is brilliant blue in pure toluene (Figure 2b). From the transmission spectra, it can be assumed that the blue color must be mainly caused by the diffuse reflection of short-wavelength visible light. The position of the peak, λ_{max}, moves to a shorter wavelength, and the peak sharpens with increasing acetone in the mixed solvent. The color of the porous gel also changes depending on the composition of the mixed solvent; the color must be generated by the diffuse reflection of visible light with wavelengths that are both shorter and longer than the peak wavelength. It is noteworthy that light of a certain wavelength range where the sharp peak can be seen in the transmission spectra can pass through this porous gel depending on the solvent composition. This optical property is

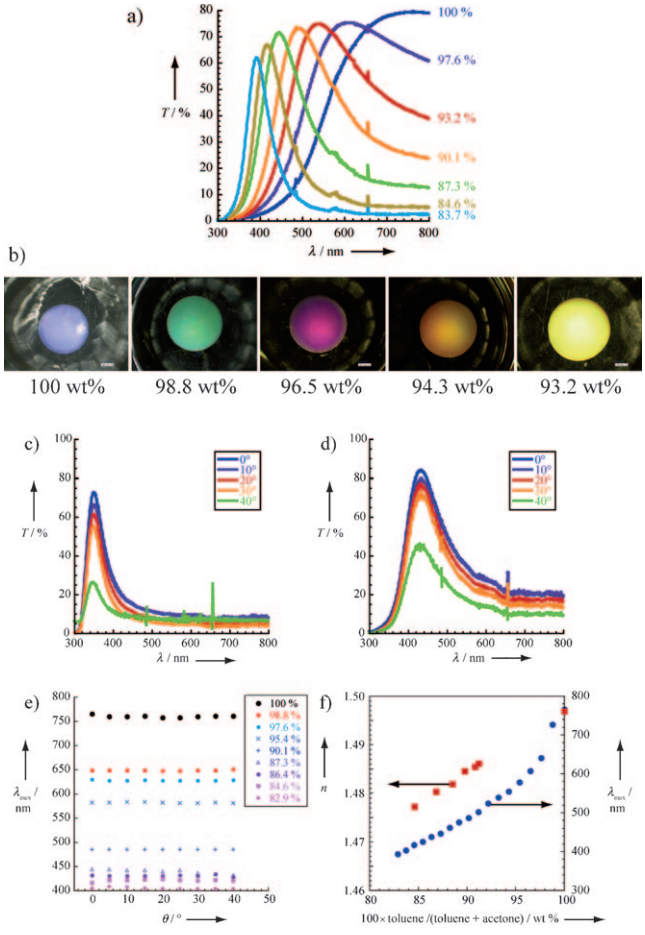

Figure 2. a) Solvent composition dependence of transmission spectra and b) optical photographs of a porous gel at 20 °C. The porous gel was prepared at 15 °C. The scale bar in (b) is 1 mm. c,d) Transmission spectra of the porous gels in different solvent compositions measured at various angles at 20 °C. The mass percentages in these figures represent the concentration of toluene in the mixed solutions. c) 75 wt% toluene, d) 85 wt% toluene. e) Plots showing λ_{max} of the transmission spectra for the porous gels in various solvent compositions versus angle at 20 °C. f) Plots showing the refractive index n of the solvents at 589 nm and λ_{max} of the transmission spectra versus the toluene compositions in the mixed solvents.

obviously different from the optical properties of the amorphous arrays prepared from submicrometer spherical particles and the nanostructures in feather barbs. A downward peak, which can be attributed to a partial photonic band gap, can be observed in the transmission spectra of the amorphous arrays. The transmission spectra measured at different angles for the porous gel in different solvent compositions are shown in Figure 2c,d. The peaks occurred at certain wavelengths depending on the solvent composition and did not depend on the angle from 0° to 40° (Figure 2e). In Figure 2f, the peak position of the spectra and the refractive indices of the mixed solvents are plotted as a function of the solvent composition. A similar tendency was observed for both changes with increasing toluene composition; the variation in the peak position is likely to be associated with the change in the refractive indices of the mixed solvents.

Temperature-dependent transmission spectra of the porous gel in pure toluene were also observed because the refractive index of the solvent is also subjected to temperature change. As shown in Figure 3a, the peak position of the spectra shifted to the shorter wavelength, and the peak becomes sharper with a rise in temperature. The refractive index of toluene and the peak position also decrease with increasing temperature (Figure 3b). Meanwhile, the swelling degrees of the porous gels remain unchanged with variations in solvent composition and temperature (Figure S8b,c in the Supporting Information), which indicates that variation in the size of the microstructure does not contribute to the change in the color.

To evaluate the contribution from the change in the refractive indices of the solvents and gel portions to the color change, the dispersion, which is a wavelength-dependent refractive index, was measured for each portion. We used poly(MEO2) [M_n (number average molecular weight) = 1.02×10^5] toluene solutions with several concentrations of the polymer in substitution for the gel portion because of the difficulties in obtaining the refractive indices of the actual gel portion. The diffuse reflection from a macroporous gel filled with a solvent requires a difference in the refractive indices between the gel portion and the solvent portion. For example, in the case that these refractive indices are different at all visible wavelengths, the porous gel diffusely reflects white light and becomes opaque. In the experimentally observed dispersion curves for most polymer solutions, except for the 10 wt% solution, the refractive indices are smaller than those in pure toluene over all visible wavelengths at 20°C (Figure 4a). However, the dispersion curve of the 10 wt% poly(MEO2) solution intersects with that of toluene at around 650 nm and 20°C. If the refractive indices of the gel portion and the solvent are equal, a certain wavelength of light around the intersection can pass through the porous gel, while the other wavelengths of light are diffusely reflected. As a result, we see the upturned peaks in the transmission spectra of the porous gel. To test this hypothesis, the dispersion curves of the 10 wt% poly(MEO2) solution and toluene at different temperatures were estimated, followed by identification of the position of the intersection between the two curves with the temperature change. Cauchy's approximate equation[20] was used to estimate the appropriate dispersion curves for each condition, based on the experimentally measured five plots of refractive indices (Figure 4b). The determined intersections between the two curves of the 10 wt% poly-

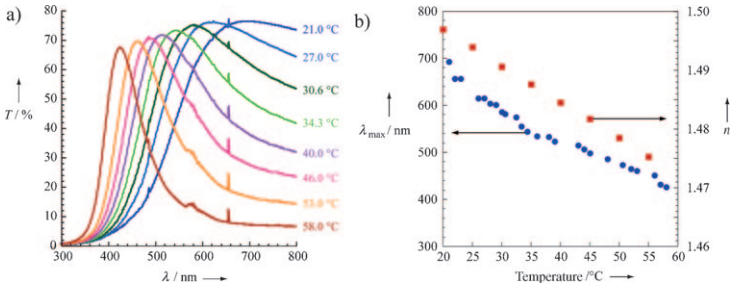

Figure 3. a) Temperature dependence of transmission spectra of the porous gel in pure toluene. The porous gel was prepared at 15°C. b) Plots showing λ_{max} of the transmission spectra of the gel in pure toluene and the refractive index n of toluene at 589 nm versus temperature.

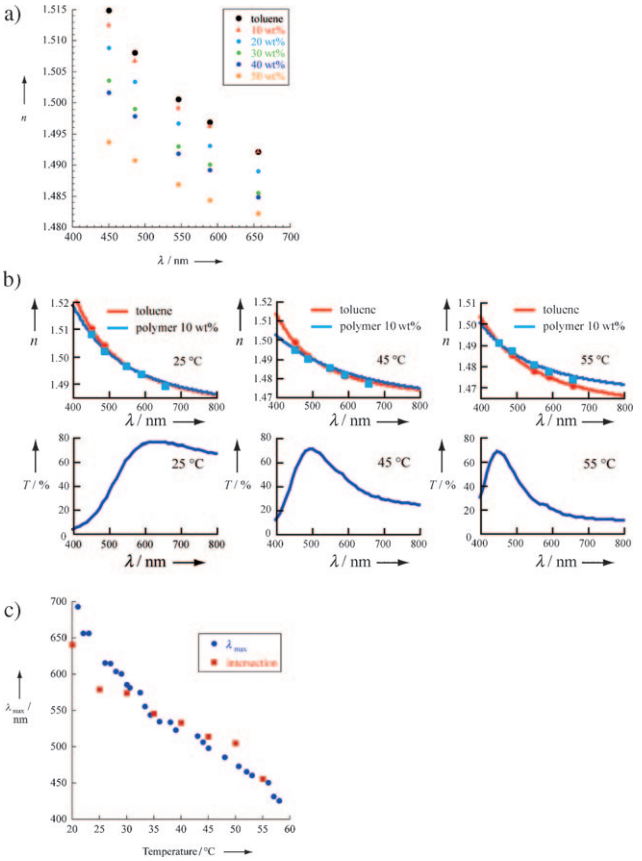

Figure 4. a) Plots showing the refractive index n of the poly(MEO2) toluene solutions with various concentrations and pure toluene depending on the wavelength at 20°C. b) Dispersion curves of pure toluene and the 10 wt% poly(MEO2) toluene solution compared at various temperatures. The intersection of these curves changed depending on temperature. The transmission spectra were obtained from the porous gel in toluene at different temperatures. c) λ_{max} of the transmission spectra of the 10 wt% poly(MEO2) toluene solution at various temperatures compared with the temperature-dependent intersections obtained by Cauchy's approximate equation.

(MEO2) solution and toluene depending on the temperature were compared to the peak wavelength of the spectra (Figure 4c) with a change in temperature. The intersections reasonably reflected the trend of the peak position of the transmission spectra with increasing temperature, which supports our hypothesis that the tunable coloration of the swollen porous gel is caused by the coincidence at one wavelength of the dispersion curves of the gel portion and the solvent portion, depending on solvent composition and temperature. Judging from Figure 4b, the sharpness of the peak must be attributed to the intersection of two dispersion curves with large angle. As a result, the porous gel exhibits brilliant colors.

So far, a few systems have been reported that use various dispersions of two different media for making optical filters.[21–29] Because, however, most systems are composed of crushed insoluble inorganic powders immersed in organic solvents or colloidal suspensions, it has been difficult to obtain structural colored membrane materials with large-scale production useful for making paperlike displays. Only Watanabe's group recently found that homogeneously prepared hydroxypropyl cellulose film exhibits colors using the similar effect when the film is swollen with solvent,[30] but the colors are subtle. In contrast, our structurally colored material generated using the phase-separation method can be obtained without difficulty, and exhibits brilliant colors: this structural colored material represents a promising new material for the manufacture of reflective full-color displays with a wide viewing angle, energy saving, and nonfading color materials. Moreover, as it has an interconnected porous structure, and also can be prepared in other stimuli-sensitive polymer systems, the newly prepared structurally colored materials should have potential as sensors and monolith systems for reactors and separation.

Experimental Section

Sample preparation: First, a 30 mL stoppered pear-shaped flask was loaded with 4,4′-dinonyl-2,2′-dipyridyl (26.2 mg) and 2-(2-methoxyethoxy) ethyl methacrylate (9.03 g). The solution was sealed with a three-way stopcock and cycled three times between nitrogen gas and vacuum to remove oxygen. Methyl 2-bromopropionate (6.69 mg) was added to the solution using a microsyringe. Next, this solution was moved using a cannula to another stoppered test tube containing CuBr (4.59 mg) and filled with nitrogen gas. The uniformly dissolved solution was divided into 1.25 mL test tubes in a globe box filled with nitrogen gas. The sealed test tubes were placed into constant-temperature baths at several temperatures, and the polymerizations proceeded for 19 h. The newly formed polymer gels were washed with acetone and obtained as clear and colorless gels or opaque gels. The preparation of linear poly(MEO2) was the same as that of the gels but the temperature and reaction time were 60 °C and 2 h, respectively. The linear polymer was purified by dialysis. The number average molecular weight of the polymer was determined by gel permeation chromatography.

Measurements: The microstructure of the gels was investigated by scanning electron microscopy (SEM, JEOL JSM 5600). The samples were coated with a 15 nm gold layer, and the microscope was operated at 10 kV. Optical photographs of the samples were taken on a digital microscope (KEYENCE VHX-500). Transmittance spectra of the samples were measured using an Ocean Optics USB 2000 fiber optic spectrometer by altering the angle of incidence from 0° to 40° within a cell whose temperature was controlled by a circulating water bath. The dispersion of the samples was measured by a multiple wavelength refractometer (ATAGO DR-M2) connected to a circulating water bath. An electronic thermometer (As One TM-300) with a precision of ±0.1 °C was used to continuously monitor the temperature of the prism of the refractometer.

Received: December 25, 2010
Published online: March 31, 2011

Keywords: color · gels · self-assembly · solvatochromism

[1] P. Vukusic, J. R. Sambles, C. R. Lawrence, *Nature* **2000**, *404*, 457–457.
[2] A. R. Parker, V. L. Welch, D. Driver, N. Martini, *Nature* **2003**, *426*, 786–787.
[3] S. Kinoshita, *Structural Colors in the Realm of Nature*, World Scientific Publishing, Shingapore, **2008**.
[4] K. Busch, S. Lölkes, R. B. Wehrspohn, *Photonic Crystals* (Ed.: H. Föll), Wiley-VCH, Weinheim, **2004**.
[5] J. J. Walish, Y. Kang, R. A. Mickiewicz, E. L. Thomas, *Adv. Mater.* **2009**, *21*, 3078–3081.
[6] M. A. Haque, G. Kamita, T. Kurokawa, K. Tsujii, J. P. Gong, *Adv. Mater.* **2010**, *22*, 5110–5114.
[7] A. C. Arsenault, D. P. Puzzo, I. Manners, G. A. Ozin, *Nat. Photonics* **2007**, *1*, 468–472.
[8] M. Harun-Ur-Rashid, T. Seki, Y. Takeoka, *Chem. Rec.* **2009**, *9*, 87–105.
[9] K. Matsubara, M. Watanabe, Y. Takeoka, *Angew. Chem.* **2007**, *119*, 1718–1722; *Angew. Chem. Int. Ed.* **2007**, *46*, 1688–1692.
[10] Y. Takeoka, M. Honda, T. Seki, M. Ishii, H. Nakamura, *ACS Appl. Mater. Interfaces* **2009**, *1*, 982–986.
[11] M. Harun-Ur-Rashid, A. Bin Imran, T. Seki, M. Ishi, H. Nakamura, Y. Takeoka, *ChemPhysChem* **2010**, *11*, 579–583.
[12] C. J. Jin, X. D. Meng, B. Y. Cheng, Z. L. Li, D. Z. Zhang, *Phys. Rev. B* **2001**, *63*, 195107.
[13] K. Edagawa, S. Kanoko, M. Notomi, *Phys. Rev. Lett.* **2008**, *100*, 013901.
[14] E. R. Dufresne, H. Noh, V. Saranathan, S. G. J. Mochrie, H. Cao, R. O. Prum, *Soft Matter* **2009**, *5*, 1792–1795.
[15] R. O. Prum, R. H. Torres, *Integr. Comp. Biol.* **2003**, *43*, 591–602.
[16] K. Matyjaszewski, J. H. Xia, *Chem. Rev.* **2001**, *101*, 2921–2990.
[17] M. Kato, M. Kamigaito, M. Sawamoto, T. Higashimura, *Macromolecules* **1995**, *28*, 1721–1723.
[18] S. Yamago, *Chem. Rev.* **2009**, *109*, 5051–5068.
[19] J. C. Stover, *Optical Scattering: Measurement and Analysis*, SPIE Optical Engineering Press, **1995**.
[20] M. Cauchy, *Philos. Mag. Ser. 3* **1941**, *8*, 459–469.
[21] C. Christiansen, *Ann. Phys. Chem.* **1884**, *23*, 298–301.
[22] G. C. Crossmon, *Anal. Chem.* **1948**, *20*, 976–977.
[23] W. C. Price, K. S. Tetlow, *J. Chem. Phys.* **1948**, *16*, 1157–1162.
[24] M. Cloupeau, S. Klarsfel, *Appl. Opt.* **1973**, *12*, 198–204.
[25] D. D. Saperstein, *J. Phys. Chem.* **1987**, *91*, 6659–6663.
[26] K. Balasubramanian, M. R. Jacobson, H. A. Macleod, *Appl. Opt.* **1992**, *31*, 1574–1587.
[27] N. J. Goddard, A. E. Maturell, *Appl. Opt.* **1995**, *34*, 7318–7320.
[28] M. Franz, B. M. Fischer, M. Walther, *Appl. Phys. Lett.* **2008**, *92–94*, 021107-1–3.
[29] T. D. Ibragimov, *J. Appl. Spectrosc.* **2009**, *76*, 752–755.
[30] S. Edo, K. Okoshi, S. Kang, M. Tokita, T. Kaneko, J. Watanabe, *Langmuir* **2010**, *26*, 1743–1746.

